SIAM J. APPL. MATH.
Vol. 68, No. 2, pp. 413–436

A HYBRID LAGRANGIAN MODEL BASED ON THE AW–RASCLE TRAFFIC FLOW MODEL*

S. MOUTARI† AND M. RASCLE†

Abstract. In this paper, we propose a simple fully discrete hybrid model for vehicular traffic flow, for which both the macroscopic and the microscopic models are based on a Lagrangian discretization of the Aw–Rascle (AR) model [A. Aw and M. Rascle, *SIAM J. Appl. Math.*, 60 (2000), pp. 916–938]. This hybridization makes use of the relation between the AR macroscopic model and a *follow-the-leader*-type model [D. C. Gazis, R. Herman, and R. W. Rothery, *Oper. Res.*, 9 (1961), pp. 545–567; R. Herman and I. Prigogine, *Kinetic Theory of Vehicular Traffic*, American Elsevier, New York, 1971], established in [A. Aw, A. Klar, M. Materne, and M. Rascle, *SIAM J. Appl. Math.*, 63 (2002), pp. 259–278]. Moreover, in the hybrid model, the total variation in space of the velocity v is nonincreasing, the total variation in space of the specific volume τ is bounded, and the total variations in time of v and τ are bounded. Finally, we present some numerical simulations which confirm that the models' synchronization processes do not affect the waves propagation.

Key words. traffic flow, hybrid model, Lagrangian discretization, macroscopic model, microscopic model, total variation

AMS subject classifications. 35L, 35L65

DOI. 10.1137/060678415

1. Introduction.

Most of the vehicular traffic models are either macroscopic [3, 12, 18, 25, 30, 33, 34, 36, 37] or microscopic [15, 22]. When following a macroscopic approach, one focuses on global parameters such as traffic density or traffic flow. In general, from a macroscopic perspective vehicular traffic is viewed as a compressible fluid flow, whereas a microscopic approach describes the behavior of each individual vehicle. Macroscopic models allow one to simulate traffic on large networks but with a poor description of the details. On the other hand, microscopic models can cover such details, but they are intractable on a large network.

However, a typical road transport system or a road network includes obstacles, different road geometries and configurations (intersections, roundabouts, multiple lanes, etc.), as well as control features, such as traffic lights and crossings, which have a nonnegligible impact on traffic in the whole network. Therefore, neither of the two approaches is separately able to capture real traffic dynamics. A natural strategy is therefore to combine macroscopic and microscopic models, depending on the number of details that we need. This *hybrid* approach has recently received a considerable interest in traffic modeling [1, 6, 8, 19, 21, 27, 31]. Indeed, such models enable one to take into account the most important details of the traffic but still allow for descriptions of the traffic on a large network. However, they require strong consistency and compatibility between macroscopic and microscopic models to be coupled [20, 31].

Here, our macroscopic description is based on the Aw–Rascle (AR) model [3], whereas the microscopic model is a *follow-the-leader* (FLM)-type model [15, 22].

*Received by the editors December 22, 2006; accepted for publication (in revised form) July 30, 2007; published electronically November 16, 2007. This work was partially supported by the former EU Network HYKE HPRN-CT-2002-00282 and by the French ACI-NIM (Nouvelles Interactions des Mathématiques) 193 (2004).

http://www.siam.org/journals/siap/68-2/67841.html

†Department de Mathématiques, Laboratoire J. A. Dieudonné, UMR CNRS 6621, Université de Nice-Sophia Antipolis, Parc Valrose, 06108 Nice Cedex 2, France (salissou@math.unice.fr, rascle@math.unice.fr).

In [2], Aw et al. established a connection between the two classes of models. More precisely, the macroscopic model can be viewed as the limit of the time discretization of a microscopic FLM-type model when the number of vehicles increases. This can be done via a (hyperbolic) scaling in space and time (zoom) for which the density and the velocity are invariant.

Our aim in the current work is to propose a simple and fully discrete hybrid model for which both the macroscopic and the microscopic parts are based on the Lagrangian discretization of the AR second order model of traffic flow.

The outline of this paper is as follows: Sections 2 and 3 provide, respectively, some details on the discretizations of the macroscopic and the microscopic models. Section 4 describes the relations between the two models. Section 5 is devoted to the presentation of the hybrid model. In section 6, we establish estimates on the total variation both in space and time for the velocity v and the specific volume τ in Lagrangian coordinates. These estimates are of course the main ingredient for studying the convergence of our hybrid scheme to a suitable initial boundary value problem, which we will investigate in a forthcoming work. Finally, in section 7, some numerical simulations of the hybrid model confirm that this micro-macro description allows for a very nice description in *both* regimes.

2. The AR macroscopic model. We are concerned with the AR macroscopic model of traffic flow. It consists of the conservative form (in Eulerian coordinates) of the two following equations:

$$\begin{cases} \partial_t \rho + \partial_x(\rho v) = 0, \\ \partial_t(\rho w) + \partial_x(\rho v w) = 0, \end{cases} \tag{2.1}$$

where ρ denotes the fraction of space occupied by cars (a dimensionless local density), v is the macroscopic velocity of cars, and, for instance, $w = v + p(\rho)$. Many other choices could be considered as well. In what follows, we will assume for concreteness that

$$p(\rho) = \begin{cases} \frac{v_{ref}}{\gamma}\left(\frac{\rho}{\rho_m}\right)^{\gamma}, & \gamma > 0, \\ -v_{ref} ln\left(\frac{\rho}{\rho_m}\right), & \gamma = 0, \end{cases} \tag{2.2}$$

with v_{ref} a given reference velocity and $\rho_m := \rho_{max} = 1$ the maximal density.

Let $\tau = 1/\rho$ be the specific volume and denote by (X, T) the Lagrangian "mass" coordinates. We have

$$\partial_x X = \rho, \qquad \partial_t X = -\rho v, \qquad T = t.$$

We recall that ρ is dimensionless; thus $X = \int^x \rho(y,t)dy$ describes the total length occupied by cars up to the point x if they were packed "nose to tail."

The system (2.1) can be rewritten in Lagrangian "mass" coordinates (X, T) as

$$\begin{cases} \partial_T \tau - \partial_X v = 0, \\ \partial_T w = 0, \end{cases} \tag{2.3}$$

now with $w = v + P(\tau) := v + p\left(\frac{1}{\tau}\right)$ (we set $\tau_m := \tau_{min} := \frac{1}{\rho_m} := \frac{1}{\rho_{max}} = 1$).

Away from the vacuum, the system (2.3) is strictly hyperbolic and is equivalent to the system (2.1). Its eigenvalues are

$$\lambda_1 = P'(\tau) < 0 \quad \text{and} \quad \lambda_2 = 0.$$

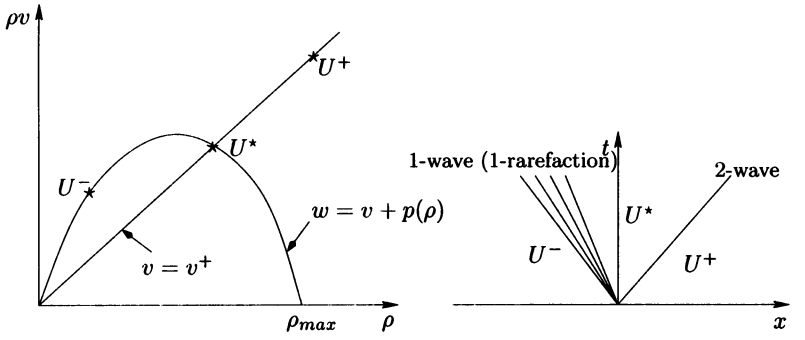

FIG. 2.1. *Riemann problem in* $(\rho, \rho v)$ *and* (x, t) *planes.*

Moreover, λ_1 is genuinely nonlinear and λ_2 is linearly degenerate. The Riemann invariants associated with the two eigenvalues λ_1 and λ_2 are v and w, respectively.

2.1. The Riemann solver. Let us consider the following Riemann problem:

$$\begin{cases} \partial_t \tau - \partial_X v = 0, \\ \partial_t w = 0, \end{cases} \tag{2.4}$$

with the initial data

$$\begin{cases} U^+(X,0) = (\tau^+, w^+) & \text{if } X > 0, \\ U^-(X,0) = (\tau^-, w^-) & \text{if } X < 0. \end{cases} \tag{2.5}$$

The natural solution $U(X,t)$ to the Riemann problem (2.4)–(2.5) involves two waves: a rarefaction or a shock wave associated with the first characteristic field λ_1 followed by a contact discontinuity associated with the second one λ_2.

PROPOSITION 2.1. *The solution of the Riemann problem* (2.4)–(2.5) *is constructed as follows. First, we connect* U^- *with an intermediate state* $U^* = (\tau^*, w^*)$ *(such that* $v^* = w^* - P(\tau^*) = v^+$ *and* $w^* = w^-$*) by a 1-shock wave (if* $v^+ < v^-$*) or a 1-rarefaction (if* $v^+ > v^-$*). Then,* U^* *is connected with* U^+ *by a 2-contact discontinuity (see Figure* 2.1*).*

Through each wave, the specific volume τ *and the velocity* v *are monotonous functions of* X/t*. Therefore, away from the vacuum, the solution* $U(X,t)$ *remains in the bounded invariant region* $\mathcal{R}$ *defined in* (2.6)*, i.e.,*

$$U(X,t) = (\tau, w), \quad \text{where } \tau = P^{-1}(w - v)$$

and

$$(v,w) \in \mathcal{R} = \{[v^{min}, v^{max}] \times [w^{min}, w^{max}]\} \cap \{w \geq v\}, \tag{2.6}$$

where $v^{min}, w^{min} \geq 0$ *and* $v^{max}, w^{max} < +\infty$ *(see Figure* 2.2*).*

In the (w,v) coordinates (see Figure 2.2) we have

$$U^\pm = (w^\pm, v^\pm) \quad \text{and} \quad U^* = (w^-, v^+). \tag{2.7}$$

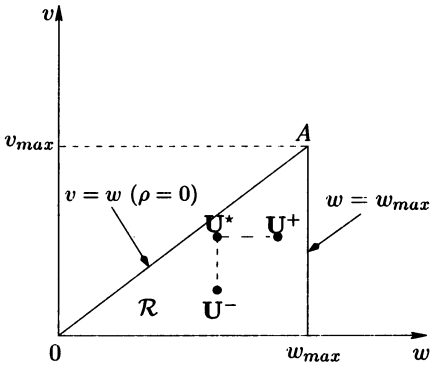

FIG. 2.2. *Riemann problem. The above triangle* $(0, A, w_{max})$ *is an invariant region in the* (w, v) *plane.*

2.2. Lagrangian discretization of the AR macroscopic model. Many approximate methods for (2.3) are based on solutions to the Riemann problem. Here, we are particularly interested in the Godunov scheme. In order to define the Godunov scheme associated with the above Riemann solver, we introduce grid points in space $X_j := j\Delta X$, $j \in \mathbb{Z}$, and in time $t_n = n\Delta t$, $n \in \mathbb{N}$. Let $h := (\Delta X, \Delta t)$ tend to $(0,0)$, with $r := \frac{\Delta t}{\Delta X} = constant$, and assume that for all $(\Delta X, \Delta t)$ the CFL condition is satisfied:

$$r \sup_{U \in \mathcal{R}} \left(\max_{i=1,2} \{|\lambda_i(U)|\} \right) \leq 1, \tag{2.8}$$

where $\mathcal{R}$ is the invariant region defined in (2.6), containing the initial data $U(x)$ for all $x \in \mathbb{R}$. Moreover, we assume that $\mathcal{R}$ does not touch the vacuum, i.e.,

$$\inf\{w - v,\ (v, w) \in \mathcal{R}\} > 0.$$

Then, the Lagrangian Godunov discretization of the AR macroscopic model (2.3) (see [2] for more details) is given by

$$\begin{cases} \tau_j^{n+1} = \tau_j^n + \frac{\Delta t}{\Delta X} \left(v_{j+1}^n - v_j^n \right), \\ w_j^{n+1} = w_j^n, \end{cases} \tag{2.9}$$

with initial data

$$\begin{cases} \tau_j(0) = \tau_j^0 \geq \frac{1}{\rho_m} = \tau_m = 1, \\ 0 \leq v_j(0) = v_j^0 \leq w_j - P(\tau_m). \end{cases} \tag{2.10}$$

PROPOSITION 2.2. *Starting with arbitrary initial data for the Godunov scheme*

$$U_h(X, 0) = (\tau_h^0, w_h^0),$$

with $(v_h^0 = w_h^0 - P(\tau_h^0), w_h^0) \in \mathcal{R}$ *(defined in (2.6)), the solutions*

$$U_h(X, t_n) = (\tau_h^n, w_h^n)$$

constructed by the Godunov scheme satisfy

$$(v_h^n = w_h^n - P(\tau_h^n), w_h^n) \in \mathcal{R}.$$

Therefore, the region $\mathcal{R}$ is also invariant for the Godunov scheme.

Proof. In each cell $I_j = [X_{j-1/2}, X_{j+1/2}]$, the variable w is constant, whereas the velocity and the specific volume τ are monotonous, by Proposition 2.1. Therefore, in each cell, $U(X,t) = (\tau, w)(X,t)$ remains in the same bounded region $\mathcal{R}$, which is thus invariant for the Godunov scheme. □

We are going to use the following results; see [4, Theorem 3.1] and [2, Theorem 1].

PROPOSITION 2.3 (see [4]). *Assume that the sequence v_h^0 is in $BV(\mathbb{R})$; that is, the total variation in space is bounded: there exists a constant $C_0 < +\infty$ such that*

$$TV_X(v_h^0; \mathbb{R}) = \sum_{j\in\mathbb{Z}} \left|v_{j+1}^0 - v_j^0\right| \le C_0.$$

Let

$$\tilde{v}_h(X,t) := v_j^n + (t - t_n)(v_j^{n+1} - v_j^n)/\Delta t \tag{2.11}$$

be the linear interpolation in time of v_h on I_j between t_n and t_{n+1} and similarly for $\tilde{\tau}_h$.

Then, for all $n \in \mathbb{N}$, for all $h = (\Delta X, \Delta t)$, we have the following:

(i) *The total variation in X of $v_h(.,t)$ is nonincreasing in time, and the total variation in t of $\tilde{v}_h(.,.)$ is bounded on $\mathbb{R} \times [0,T]$:*

$$\begin{aligned} \sup_{t\ge 0} TV_X(v_h(.,t)) &= \sup_{n\in\mathbb{N}} TV_X(v_h^n; \mathbb{R}) \\ &= \sup_{n\in\mathbb{N}} \sum_{j\in\mathbb{Z}} \left|v_{j+1}^n - v_j^n\right| \le TV_X(v_h^0, \mathbb{R}) \le C_0, \end{aligned} \tag{2.12}$$

$$TV_t(\tilde{v}_h(.,.); \mathbb{R} \times [t,t']) \le C \max(|t' - t|, \Delta t) C_0. \tag{2.13}$$

(ii) *The total variation in X of $\tau_h(.,t)$ on $\cup_{j\in\mathbb{Z}} I_j$ and the total variation in t of $\tilde{\tau}_h(.,.)$ on $\mathbb{R} \times [0,\infty]$ are bounded uniformly in h; i.e., there exists a constant C' independent of h such that*

$$\sup_h \sup_{t\ge 0} \sum_{j\in\mathbb{Z}} TV_X(\tau_h(.,t); I_j) \le C' C_0, \tag{2.14a}$$

$$\forall t \in [0,t'],\ \sup_h TV_t(\tilde{\tau}_h(.,.); \mathbb{R} \times [t,t']) \le C' \max(|t' - t|, \Delta t) C_0. \tag{2.14b}$$

We recall that I_j is the open interval $\left(X_{j-1/2}, X_{j+1/2}\right)$. Moreover, if we assume that w_h and τ_h are initially in $BV(\mathbb{R})$, then (2.14a) *can be replaced by the stronger result*

$$\sup_h \sup_{t\ge 0} TV_X(\tau_h(.,t); \mathbb{R}) \le C' C_0. \tag{2.15}$$

3. The microscopic (FLM) model. The microscopic model that we consider is an FLM-type model [15, 22]. In such a model, the basic idea is that the acceleration at time t depends on the relative speeds of the vehicle and its leading vehicle at time t as well as the distance between the vehicles. Therefore, the dynamics of a vehicle j is given by the two equations

$$\begin{cases} \frac{dx_j}{dt} = v_j, \\ \frac{dv_j}{dt} = P'\left(\frac{x_{j+1} - x_j}{\Delta X}\right)\left(\frac{v_{j+1} - v_j}{\Delta X}\right), \end{cases} \tag{3.1}$$

where $x_j(t)$ and $v_j(t)$ are, respectively, the position and the velocity of the vehicle j at time t, and ΔX is its length. Here, $\rho_j := \frac{\Delta X}{(x_{j+1}-x_j)}$ is the normalized local density (more precisely the fraction of space occupied by a vehicle) of this vehicle. Therefore, the specific volume is $\tau_j = \frac{1}{\rho_j} = \frac{(x_{j+1}-x_j)}{\Delta X}$ and the maximal density $\rho_m = \rho_{max} = \frac{1}{\tau_m} = 1 := \frac{1}{\tau_{min}}$. In this section, contrarily to sections 5 and 6, the car $(j+1)$ is the leader of car j. A prototype is the case where $P(\tau) = p\left(\frac{1}{\tau}\right) = \frac{v_{ref}}{\gamma}\left(\frac{\rho}{\rho_m}\right)^{\gamma}$ (with v_{ref} a given reference velocity and $\gamma > 0$ a given parameter) and $w_j = v_j + P(\tau_j)$. Then system (3.1) writes

$$\begin{cases} \frac{d\tau_j}{dt} = \frac{(v_{j+1}-v_j)}{\Delta X}, \\ \frac{dw_j}{dt} = 0. \end{cases} \tag{3.2}$$

The explicit first order Euler time discretization (with step Δt of system (3.2) is then

$$\begin{cases} \tau_j^{n+1} = \tau_j^n + \frac{\Delta t}{\Delta X}\left(v_{j+1}^n - v_j^n\right), \\ w_j^{n+1} = w_j^n, \end{cases} \tag{3.3}$$

with

$$v_j^{n+1} = w_j^{n+1} - P(\tau_j^{n+1})$$

and initial conditions

$$\begin{cases} \tau_j(0) = \tau_j^0 \geq \frac{1}{\rho_m} = \tau_m = 1, \\ 0 \leq v_j(0) = v_j^0 \leq w_j - P(\tau_m). \end{cases} \tag{3.4}$$

As in the macroscopic scheme, we can define $(\tilde{\tau}_h, \tilde{v}_h)$ by (2.11). Since system (3.3) is *exactly* the same as (2.9), $\tilde{\tau}_h$ and $\tilde{v}_h$ satisfy the same BV estimates as in Proposition 2.3.

4. Link between the macroscopic and microscopic model: The scaling. We now consider a large number of vehicles on a long stretch of road. Let us now introduce in the AR macroscopic model (2.3) a scaling (zoom) such that the size of the considered domain and the number of vehicles tend to infinity, whereas the vehicle length tends to 0. Let ϵ be the scaling parameter. For some given Eulerian or Lagrangian coordinates (x,t) or (X,t), we consider the rescaled coordinates

$$(x',t') = (\epsilon x, \epsilon t); \qquad (X',t') = (\epsilon X, \epsilon t).$$

Consequently, the length of a vehicle is now $\Delta X' = \epsilon \Delta X$. The parameter ϵ is proportional to the inverse of maximal possible number of vehicles per new unit length. However, in the new coordinates (X',t'), the variable τ (resp., ρ) and the Riemann invariant (v,w) remain unchanged, that is,

$$\tau' = \tau \text{ (resp., } \rho' = \rho), \quad v' = v, \quad w' = w.$$

Thus the system (2.3) becomes

$$\begin{cases} \frac{\partial \tau}{\partial t} = \frac{\partial v}{\partial X'}, \\ \frac{\partial w}{\partial t'} = 0. \end{cases} \tag{4.1}$$

Using the same scaling for the microscopic model, (3.2) now writes

$$\begin{cases} \frac{d\tau_j}{dt'} = \frac{1}{\Delta X'}\,(v_{j+1} - v_j)\,, \\ \frac{dw_j}{dt'} = 0. \end{cases} \tag{4.2}$$

Both in the original and in the rescaled coordinates, the standard first order explicit Euler discretization of the microscopic model (3.3) is equivalent to the Godunov discretization (2.9) of the macroscopic model; see (7.1), (7.2), (7.3), and (7.4).

5. Hybrid Lagrangian model. In order to construct our hybrid Lagrangian model, we want to combine a macroscopic description away from the junctions, traffic lights, etc. and a microscopic view near these obstacles as shown in Figure 5.1.

Thanks to the equivalence established above between the two models, we expect to get rid of the usual compatibility problems encountered when developing a hybrid model.

5.1. Description of the two Lagrangian models. Since the macroscopic model is shown to be the limit of a large number of vehicles on a long stretch of road (away from the vacuum), we may consider that a Lagrangian macroscopic (moving) cell (or the corresponding moving Eulerian cell) contains a "*long vehicle*" made by juxtaposition of *several (say N) ordinary vehicles*, whereas in the microscopic model, a Lagrangian cell contains a *single ordinary vehicle*, as depicted in Figure 5.1. Obviously macroscopic Lagrangian cells are much larger than microscopic ones. In Eulerian hybrid models (see, e.g., [6, 8, 19, 21, 27, 31]), the "microscopic region" is fixed in Eulerian coordinates. In contrast, here, this "actual microscopic region (AMR)" (see Figure 5.1) is piecewise constant in Lagrangian coordinates. It is moving in Eulerian coordinates and is periodically refreshed in order to *always* contain a *fixed* Eulerian region: the "minimal microscopic region (MMR)" (see Figure 5.1) around the junction, traffic light, etc., in which our description will *always* be microscopic.

5.2. Model synchronization. In this section we show in detail how to pass from the macroscopic to the microscopic description and vice versa. Here and in the next sections, we order the cells and the cars by calling $(i-1)$ the leader and i the follower.

5.2.1. From the macroscopic to the microscopic model. When a macroscopic Lagrangian cell enters the MMR, we split the "*long vehicle*" (which is nothing but a juxtaposition of N cars) into N different microscopic cells and uniformly distribute these cars over the length L of the macroscopic cell, as shown in Figure 5.2. Here, all our vehicles are supposed to have the same length. In principle, we could also cover the case of vehicles with different lengths; see Remark 5.1 below.

This splitting does not modify the specific volume τ. Indeed, in the macroscopic

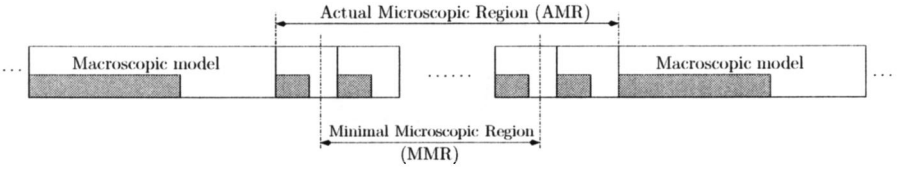

FIG. 5.1. *Hybrid Lagrangian model.*

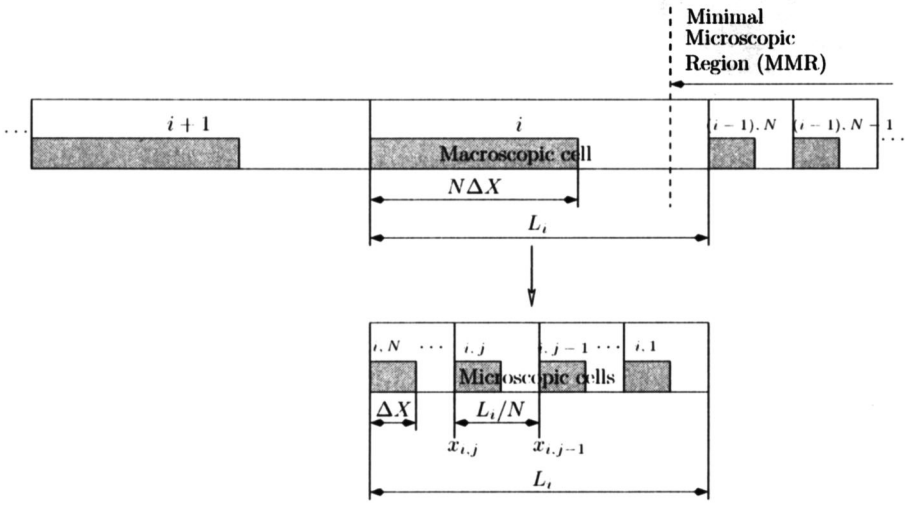

FIG. 5.2. *From the macroscopic to the microscopic model: before (above) and after (below) the synchronization.*

cell i, we have

$$\tau_i = \frac{L_i}{N\Delta X} = \tau_{mac}. \tag{5.1}$$

When this cell i becomes microscopic, the distance between two successive cars (i,j) (the follower) and $(i,j-1)$ (the leader) is

$$(x_{i,j-1} - x_{i,j}) = \frac{L_i}{N}. \tag{5.2}$$

Therefore, the microscopic specific volume in each of these microscopic cells is now

$$\tau_{i,j} = \tau_{mic} = \frac{L_i/N}{\Delta X} = \tau_{mac}. \tag{5.3}$$

So the specific volume does not change when passing from the macroscopic to the microscopic model. Notice that in the Godunov scheme the Lagrangian variable w does not change in time inside a cell i: $w_{i,j}^{n+1} = w_{i,j}^n$. Therefore, in the microscopic cells $w_{i,j}$ will be the same as in the macroscopic cell, i.e., $w_{i,j} = w_i$. Consequently, the velocity also does not change:

$$v_{i,j} = w_{i,j} - P(\tau_{i,j}) = w_i - P(\tau_i) = v_i \quad \text{for all microscopic cars } j \text{ in this cell } i.$$

REMARK 5.1. *In the case of vehicles with different lengths, we need to keep the order of vehicles and their respective lengths in each macroscopic cell. Since there is no possibility of overtaking (our model is in principle a one lane model), this order remains constant in time. Let us consider a macroscopic cell i of total length L_i and let $\Delta X_{i,j}$ be the length of the microscopic vehicle j in this cell. When this cell becomes microscopic, we need to distribute uniformly the cars over the length L_i. In the synchronization macro-micro, we distribute uniformly the specific volume among all the vehicles of this cell:*

$$\tau_{i,j} = \tau_{mic} = \frac{x_{i,j-1} - x_{i,j}}{\Delta X_{i,j}} = \tau_i = \frac{L_i}{\sum_{j=1}^{N} \Delta X_{i,j}} = \tau_{mac} \quad \forall\, j = 1, \ldots, N. \tag{5.4}$$

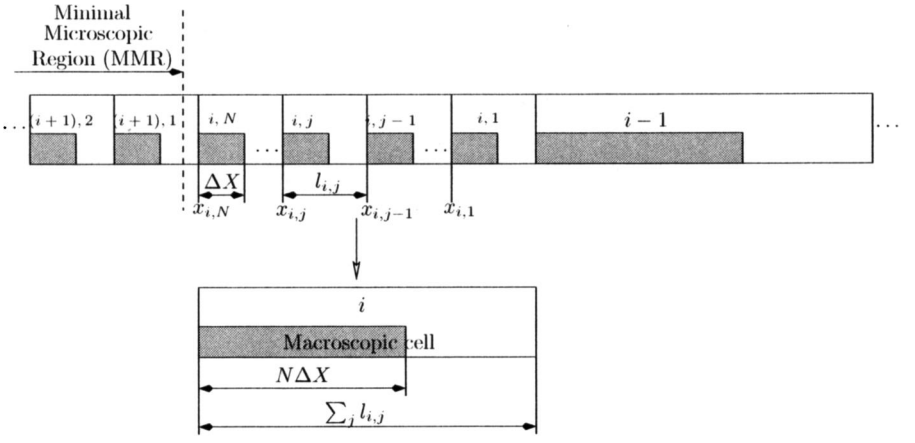

FIG. 5.3. *From the microscopic to the macroscopic model: before (above) and after (below) the synchronization.*

Therefore, we compute the distance $l_{i,j} = (x_{i,j-1} - x_{i,j})$ *for all* $j = 2, \dots, N$ *by solving the following system:*

$$\begin{cases} \frac{l_{i,j}}{\Delta X_{i,j}} = \frac{l_{i,j-1}}{\Delta X_{i,j-1}} & \forall\ j = 1, \dots, N, \\ \sum_{j=1}^{n} l_{ij} = L_i. \end{cases} \tag{5.5}$$

5.2.2. From the microscopic to the macroscopic model. When the last (say the (i, N)th) vehicle has completely left the MMR, we do exactly the converse; i.e., we aggregate the N vehicles to form a new macroscopic "*vehicle.*" We set $l_{i,j} = x_{ij-1} - x_{i,j}$, with $x_{i,j}$ the position of vehicle (i, j) as indicated in Figure 5.3.

The macroscopic specific volume will be

$$\bar{\tau}_i = \frac{\sum_{j=1}^{N} l_{i,j}}{N\Delta X} = \frac{1}{N}\sum_{j=1}^{N} \frac{l_{i,j}}{\Delta X} = \frac{1}{N}\sum_{j=1}^{N} \tau_{i,j}. \tag{5.6}$$

The Lagrangian variable $w_{i,j}$ is conserved, since according to subsection 5.2.1 the N vehicles have the same Lagrangian variable $w_{i,j} = w_i$. Thus, averaging in Lagrangian coordinates, we have

$$\frac{1}{N}\sum_{j=1}^{N} w_{i,j} = \frac{1}{N}\sum_{j=1}^{N} w_i = w_i. \tag{5.7}$$

Therefore, the corresponding macroscopic velocity is $\bar{v}_i = w_i - P(\bar{\tau}_i)$.

In this case, the macroscopic model does not inherit exactly the microscopic parameters but only the average values for τ and w and the above corresponding velocity. In spite of this change of parameters, we will prove in the following section that in the hybrid model the total variation in space of v is nonincreasing, the total variation in space of τ is bounded, and total variations in time of v and τ are bounded.

6. Estimates on the total variation in the hybrid model. In this section, with the above synchronizations between the macroscopic and the microscopic models,

we show that in the hybrid model the total variation in space of the velocity v is nonincreasing, the total variation in space of the specific volume τ is bounded, and the total variations in time of v and τ are bounded.

First, the following type of results is classical. Its proof is recalled below for the convenience of the reader.

LEMMA 6.1. *Let* $U = (u_1, u_2, \dots, u_n) \in \mathbb{R}^n$ *and* $\bar{u} \in \mathbb{R}$ *such that*

$$m = \min_i(u_i) \le \bar{u} \le \max_i(u_i) = M.$$

Then,

$$\forall\, \alpha, \beta \in \mathbb{R}, \quad |\alpha - \bar{u}| + |\bar{u} - \beta| \le |\alpha - u_1| + \sum_{i=1}^{n-1} |u_i - u_{i+1}| + |u_n - \beta|\,. \tag{6.1}$$

Proof.

$$\begin{aligned} |\alpha - \bar{u}| + |\bar{u} - \beta| &= |\alpha - u_1 + u_1 - \bar{u}| + |\bar{u} - u_n + u_n - \beta| \\ &\le |\alpha - u_1| + |u_1 - \bar{u}| + |\bar{u} - u_n| + |u_n - \beta|\,. \end{aligned} \tag{6.2}$$

Now let us prove that $|u_1 - \bar{u}| + |\bar{u} - u_n| \le \sum_{i=1}^{n-1} |u_i - u_{i+1}| = TV(u_i)_{i=1,\dots,n}$.

Since the function $\{\bar{u} \longmapsto |u_1 - \bar{u}| + |\bar{u} - u_n|\}$ is convex, its maximum is attained at an extremum point u_k equal to m or M; therefore,

$$\begin{aligned} |u_1 - \bar{u}| + |\bar{u} - u_n| &\le \max\left(|u_1 - M| + |M - u_n|\,, |u_1 - m| + |m - u_n|\right) \\ &\le |u_1 - u_k| + |u_k - u_n| \\ &\le |u_1 - u_2| + \cdots + |u_{k-1} - u_k| \\ &\quad + |u_k - u_{k+1}| + \cdots + |u_{n-1} - u_n| \\ &= \sum_{i=1}^{n-1} |u_i - u_{i+1}| = TV(u_i)_{i=1,\dots,n}. \qquad \square \end{aligned} \tag{6.3}$$

Let us denote by v_i^n (resp., τ_i^n) and $v_{i,j}^n$ (resp., $\tau_{i,j}^n$), respectively, the macroscopic and the microscopic velocities (resp., specific volumes) at time t_n. At time $t = 0$, the velocities are in $BV(\mathbb{R})$ in both models and therefore in the hybrid one.

According to sections 2 and 3, the results of Proposition 2.3 hold, in both the macroscopic and the microscopic models, away from the synchronized cells. Therefore, we focus on the synchronization process, i.e., when passing from one representation to another.

Passing from a macroscopic cell to several microscopic cells does not change the velocity and the specific volume and therefore does not change their total variation.

On the other hand, when we convert N microscopic cells into a macroscopic one, the total variation of the hybrid model can change. We are going to show that nevertheless the total variation in space of the velocity v is nonincreasing, the total variation in space of the specific volume τ is bounded, and the total variations in time of v and τ are bounded.

Let us denote by TV_X and TV_X' the total variation in space, respectively, before and after this *micro-macro* synchronization. Since inside the synchronized cell (say $\bar{I}_{sync} = \bar{I}_i$), $\bar{\tau} = \frac{1}{N}\sum_j^N \tau_j$, $\bar{v} = w - P(\bar{\tau})$, and P is nonincreasing, we have, by

Lemma 6.1,

$$\begin{aligned} TV'_X(\tau_h(.,t_n),\bar{I}_{sync}) &= \left|\tau^n_{i-1}-\bar{\tau}^n_i\right|+\left|\bar{\tau}^n_i-\tau^n_{i+1,1}\right| \\ &\le \left|\tau^n_{i-1}-\tau^n_{i,1}\right|+\sum_{j=1}^{N-1}\left|\tau^n_{i,j}-\tau^n_{i,j+1}\right|+\left|\tau^n_{i,N}-\tau^n_{i+1,1}\right| \\ &= TV_X(\tau_h(.,t_n),\bar{I}_{sync}), \end{aligned} \tag{6.4}$$

and similarly

$$\begin{aligned} TV'_X(v_h(.,t_n),\bar{I}_{sync}) &= \left|v^n_{i-1}-\bar{v}^n_i\right|+\left|\bar{v}^n_i-v^n_{i+1,1}\right| \\ &\le \left|v^n_{i-1}-v^n_{i,1}\right|+\sum_{j=1}^{N-1}\left|v^n_{i,j}-v^n_{i,j+1}\right|+\left|v^n_{i,N}-v^n_{i+1,1}\right| \\ &= TV_X(v_h(.,t_n),\bar{I}_{sync}). \end{aligned} \tag{6.5}$$

Therefore, after any (micro-macro or conversely) synchronization process, the total variation *in space* of v is nonincreasing and the total variation *in space* of τ is bounded:

$$TV'_X(v_h(.,t_n),\bar{I}_{sync}) \le TV_X(v_h(.,t_n),\bar{I}_{sync}). \tag{6.6}$$

We recall that in each macroscopic cell i, v_h and τ_h are monotonous in time in $[t_n,t_{n+1})$, that is,

$$\min(v^n_i,v^n_{i+1}) \le v^{n+1}_i \le \max(v^n_i,v^n_{i+1}), \tag{6.7}$$

and similarly for τ. Therefore, v_h,τ_h and their linear interpolations in time $\tilde{v}_h,\tilde{\tau}_h$ defined in (2.11) satisfy (2.14a) (or (2.15)) and (2.14b); see Proposition 2.3.

Moreover, as we said in sections 3 and 4, the macroscopic and microscopic models are essentially the same. In particular, the same BV estimates hold in microscopic cells for $(\tilde{v}_h,\tilde{\tau}_h)$.

According to the monotonicity property of v (see (6.7)), we have

$$\left|v^{n+1}_i-v^n_{i+1}\right|+\left|v^n_i-v^{n+1}_i\right| = \left|v^n_{i+1}-v^n_i\right|. \tag{6.8}$$

Let us denote, respectively, by $\mathcal{M}^n$ and μ^n the sets of indices of macroscopic cells and discretized macroscopic cells (i.e., split into microscopic cells) at time t_n. Therefore, $\mathcal{M}^n \cup \mu^n = \mathbb{Z}$.

From (6.6) and (6.8) we have

$$TV_X(v_h(.,t_n),\mathbb{R}) \le TV_X(v_h(.,t_{n-1}),\mathbb{R}) \le \cdots \le TV_X(v^0_h,\mathbb{R}) = C_0. \tag{6.9}$$

In each cell I_k, $\tau_h(X,t) = P^{-1}(w_k - v_h(X,t))$, with P^{-1} Lipschitz-continuous. Therefore,

$$TV_X(\tau_h(.,t_n),\{\cup I_k; k\in\mathcal{M}^n\cup\mu^n\}) = \sum_{k\in\mathcal{M}^n\cup\mu^n} TV_X(\tau_h(.,t_n),I_k) \le C_1C_0, \tag{6.10}$$

where $C_1 := \left\|(P^{-1})'\right\|_{L^\infty}$.

Now let us study how the total variation in time evolves in our hybrid model:

$$TV_t(\tilde{\tau}_h(.,.);\mathbb{R}\times[t,t']) \le \sum_{t-\Delta t\le n\Delta t\le t'+\Delta t} (A_n+B_n+C_n+D_n), \tag{6.11}$$

with

$$A_n = \sum_{i \in \mathcal{M}^n \cap \mathcal{M}^{n-1}} \left|\tau_i^n - \tau_i^{n-1}\right| N\Delta X,$$

$$B_n = \sum_{i \in \mu^n \cap \mu^{n-1}} \sum_{j=1}^{N} \left|\tau_{ij}^n - \tau_{ij}^{n-1}\right| \Delta X,$$

$$C_n = \sum_{i \in \mu^n \cap \mathcal{M}^{n-1}} \sum_{j=1}^{N} \left|\tau_{ij}^n - \tau_i^{n-1}\right| \Delta X,$$

$$D_n = \sum_{i \in \mathcal{M}^n \cap \mu^{n-1}} \sum_{j=1}^{N} \left|\bar{\tau}_i^n - \tau_{ij}^{n-1}\right| \Delta X.$$

Note that in (6.11) the summation involves all the times $t = n\Delta t$ between times t and t'.

We recall that we have, respectively, in the macroscopic model (see (2.9)) and the microscopic model (see (3.3)) the following:

(6.12a) $$\tau_i^n = \tau_i^{n-1} - \frac{\Delta t}{N\Delta X}\left(v_{i+1}^{n-1} - v_i^n\right) \text{ and}$$

(6.12b) $$\tau_{ij}^n = \tau_{ij}^{n-1} - \frac{\Delta t}{\Delta X}\left(v_{ij+1}^{n-1} - v_{ij}^n\right),$$

$$\begin{aligned} A_n &= \Delta t \sum_{i \in \mathcal{M}^n \cap \mathcal{M}^{n-1}} \left|v_{i+1}^{n-1} - v_i^n\right| \text{ by (6.12a)} \\ &\le \Delta t \sum_{i \in \mathcal{M}^n \cap \mathcal{M}^{n-1}} \left|v_{i+1}^{n-1} - v_i^{n-1}\right| \text{ due to (6.7)} \\ &\le \Delta t \sum_{i \in \mathbb{Z}} \left|v_{i+1}^{n-1} - v_i^{n-1}\right| \\ &= \Delta t\, TV_X(v_h(.,t_{n-1}), \mathbb{R}) \le \Delta t\, TV_X(v_h^0, \mathbb{R}) = \Delta t C_0, \end{aligned}$$

$$\begin{aligned} B_n &= \Delta t \sum_{i \in \mu^n \cap \mu^{n-1}} \sum_{j=1}^{N} \left|v_{ij+1}^{n-1} - v_{ij}^n\right| \text{ by (6.12b)} \\ &\le \Delta t \sum_{i \in \mu^n \cap \mu^{n-1}} \sum_{j=1}^{N} \left|v_{ij+1}^{n-1} - v_{ij}^{n-1}\right| \text{ due to (6.7)} \\ &\le \Delta t \sum_{i \in \mathbb{Z}} \sum_{j=1}^{N} \left|v_{ij+1}^{n-1} - v_{ij}^{n-1}\right| \\ &= \Delta t\, TV_X(v_h(.,t_{n-1}), \mathbb{R}) \le \Delta t\, TV_X(v_h^0, \mathbb{R}) = \Delta t C_0, \end{aligned}$$

$$\begin{aligned} C_n &= \Delta X \sum_{i \in \mu^n \cap \mathcal{M}^{n-1}} \sum_{j=1}^{N} \left|\tau_{ij}^n - \tau_i^{n-1}\right| \\ &\le \Delta X \sum_{i \in \mu^n \cap \mathcal{M}^{n-1}} \sum_{j=1}^{N} \left(\left|\tau_{ij}^n - \tau_{ij}^{n-1}\right| + \left|\tau_{ij}^{n-1} - \tau_i^{n-1}\right|\right) \end{aligned}$$

$$= \Delta X \sum_{i \in \mu^n \cap \mathcal{M}^{n-1}} \sum_{j=1}^{N} \left| \tau_{ij}^n - \tau_{ij}^{n-1} \right| \text{ (since } \tau_{ij}^{n-1} = \tau_i^{n-1},$$

according to the macro-micro synchronization process)

$$= \Delta t \sum_{i \in \mu^n \cap \mathcal{M}^{n-1}} \sum_{j=1}^{N} \left| v_{ij+1}^{n-1} - v_{ij}^n \right|$$

$$\leq \Delta t \sum_{i \in \mu^n \cap \mathcal{M}^{n-1}} \sum_{j=1}^{N} \left| v_{ij+1}^{n-1} - v_{ij}^{n-1} \right| \text{ due to (6.7)}$$

$$\leq \Delta t \sum_{i \in \mathbb{Z}} \sum_{j=1}^{N} \left| v_{ij+1}^{n-1} - v_{ij}^{n-1} \right|$$

$$= \Delta t \; TV_X(v_h(., t_{n-1}), \mathbb{R}) \leq \Delta t \; TV_X(v_h^0, \mathbb{R}) = \Delta t C_0,$$

$$D_n = \Delta X \sum_{i \in \mathcal{M}^n \cap \mu^{n-1}} \sum_{j=1}^{N} \left| \bar{\tau}_i^n - \tau_{ij}^{n-1} \right|$$

$$\leq \Delta X \sum_{i \in \mathcal{M}^n \cap \mu^{n-1}} \sum_{j=1}^{N} \left| \bar{\tau}_i^n - \tau_{ij}^n \right| + \Delta X \sum_{i \in \mathcal{M}^n \cap \mu^{n-1}} \sum_{j=1}^{N} \left| \tau_{ij}^n - \tau_{ij}^{n-1} \right|$$

$$=: D_n^1 + D_n^2,$$

$$D_n^1 = \Delta X \sum_{i \in \mathcal{M}^n \cap \mu^{n-1}} \sum_{j=1}^{N} \left| \bar{\tau}_i^n - \tau_{ij}^n \right|$$

$$\leq \Delta X \sum_{i \in \mathcal{M}^n \cap \mu^{n-1}} N \max_j \left| \bar{\tau}_i^n - \tau_{ij}^n \right|$$

$$\leq N \Delta X \sum_{i \in \mathcal{M}^n \cap \mu^{n-1}} \left| \tau_{ir}^n - \tau_{is}^n \right|,$$

$$\left(\text{since } \min_j(\tau_{ij}^n) = \tau_{is}^n \leq \bar{\tau}_i^n \leq \max_j(\tau_{ij}^n) = \tau_{ir}^n\right)$$

$$\leq N \Delta X \; TV_X(\tau_h(., t_n), \cup_{i \in \mathbb{Z}} I_i) \text{ by the same argument as in}$$

the proof of Lemma 6.1

$$\leq N \Delta X \; TV_X(v_h^0, \mathbb{R}) \left\| (P^{-1})' \right\|_{L^\infty} = N \Delta X C_1 C_0 \text{ due to (6.10)},$$

$$D_n^2 = \Delta X \sum_{i \in \mathcal{M}^n \cap \mu^{n-1}} \sum_{j=1}^{N} \left| \tau_{ij}^n - \tau_{ij}^{n-1} \right|$$

$$= \Delta t \sum_{i \in \mathcal{M}^n \cap \mu^{n-1}} \sum_{j=1}^{N} \left| v_{ij+1}^{n-1} - v_{ij}^n \right|$$

$$\leq \Delta t \sum_{i \in \mathcal{M}^n \cap \mu^{n-1}} \sum_{j=1}^{N} \left| v_{ij+1}^{n-1} - v_{ij}^{n-1} \right| \text{ due to (6.7)}$$

$$\leq \Delta t \sum_{i\in\mathbb{Z}} \sum_{j=1}^{N} \left| v_{ij+1}^{n-1} - v_{ij}^{n-1} \right|$$
$$= \Delta t \; TV_X(v_h(.,t_{n-1}),\mathbb{R}) \leq \Delta t \; TV_X(v_h^0,\mathbb{R}) = \Delta t C_0.$$

So, $D_n \leq N\Delta X C_1 C_0 + \Delta t C_0$.

Finally, we get

$$TV_t(\tilde{\tau}_h(.,.);\mathbb{R}\times[t,t']) \leq (|t'-t| + 2\Delta t)(N\Delta X C_1 + 4\Delta t)C_0. \tag{6.13}$$

We recall that we study the limit when $\frac{\Delta t}{\Delta X}$ is constant and satisfies the CFL condition (2.8).

In each cell, the specific volume τ_h is monotonous, w_h is constant, and the velocity is

$$v_h = w_h - P(\tau_h),$$

where P is a monotonous Lipschitz continuous function. Therefore, there exists a $C_2 < +\infty$ such that

$$TV_t(\tilde{v}_h(.,.);\mathbb{R}\times[t,t']) \leq (|t'-t| + 2\Delta t)C_2 C_0. \tag{6.14}$$

We summarize the above results in the following.

THEOREM 6.2. *Assume that the sequences (v_h^0, τ_h^0), respectively, the initial data for v and τ (and therefore for w), are in $BV(\mathbb{R})$; i.e., there exist some constants $c_v < +\infty$ and $c_\tau < +\infty$ such that*

$$TV_X(v_h^0;\mathbb{R}) = \sum_{i\in\mathcal{M}^0} \left| v_i^0 - v_{i+1}^0 \right| + \sum_{i\in\mu^0} \sum_{j=1}^{N} \left| v_{ij}^0 - v_{ij+1}^0 \right| + b_v \leq c_v, \tag{6.15}$$

$$TV_X(\tau_h^0;\mathbb{R}) = \sum_{i\in\mathcal{M}^0} \left| \tau_i^0 - \tau_{i+1}^0 \right| + \sum_{i\in\mu^0} \sum_{j=1}^{N} \left| \tau_{ij}^0 - \tau_{ij+1}^0 \right| + b_\tau \leq c_\tau, \tag{6.16}$$

where b_v and b_τ are the boundary terms (for instance $b_v = \sum \left| v_k^0 - v_{lj}^0 \right|$ with $k \in \mathcal{M}^0$ and $l = k \pm 1 \in \mu^0$).

Moreover, assume that the CFL condition (2.8) is satisfied and let Δt, ΔX, and $N\Delta X$ be constant with $\frac{\Delta t}{\Delta X}$ = constant. Then, the following hold:

(i) *In the macroscopic region (2.9) (resp., the microscopic region (3.3)), we have the following (see [2, 4]):*
   (a) *the total variation in X of $v_h(.,t)$ (resp., in t of $\tilde{v}_h(.,.)$ and therefore of $v_h(.,.)$) is nonincreasing in time (resp., is bounded on $\mathbb{R}\times[t,t']$);*
   (b) *the total variation in X of $\tau_h(.,t)$ on $\cup_{j\in\mathbb{Z}} I_j$ (resp., in t of $\tilde{\tau}_h(.,.)$ and therefore of $\tau_h(.,.)$, on $\mathbb{R}\times[t,t']$) is bounded (resp., is bounded).*

(ii) *During the synchronization process, at each time t_n, the total variations in X of v_h and τ_h do not increase and their total variations in time are controlled from above.*

(iii) *Therefore, in the whole hybrid model we have the following:*
   (a) *the total variation in X of $v_h(.,t)$ (resp., in t of $\tilde{v}_h(.,.)$ and therefore of $v_h(.,.)$) is nonincreasing in time thanks to (6.9) (resp., is bounded on $\mathbb{R}\times[t,t']$ thanks to (6.14));*

(b) *the total variation in* X *of* $\tau_h(.,t)$ *on* $\cup_{j\in\mathbb{Z}} I_j$ *(resp., in* t *of* $\tilde{\tau}_h(.,.)$ *and therefore of* $\tau_h(.,.)$ *on* $\mathbb{R}\times[t,t')$*) is bounded thanks to* (6.10) *(resp., is bounded thanks to* (6.13)*).*

We are now in position to establish the convergence of the discrete solution constructed by our hybrid scheme. Let us first recall the following.

DEFINITION 6.3 (see [2, 4]).

(i) *An* L^∞ *function*

$$U := (\tau, w) : \mathbb{R}\times\mathbb{R}_+ \longrightarrow \mathbb{R}^2$$

is called a weak entropy solution to the Lagrangian system (2.3) *if it is a weak solution (see* (ii)*) and if for any entropy-flux pair* $(\eta(\tau,w), q(\tau,w))$ *with* $\eta(\tau,w)$ *convex in* τ*, and for any* $\phi(X,t)\in C_0^\infty(\mathbb{R}\times\mathbb{R}_+)$*,* $\phi\geq 0$*, we have*

$$\int_0^\infty\int_{\mathbb{R}} (\eta(U)\partial_t\phi + q(U)\partial_X\phi)dXdt + \int_{\mathbb{R}}\eta(U_0(X))\phi(X,0)dX \geq 0. \tag{6.17}$$

(ii) U *is called a weak solution to* (2.3) *if the above inequality holds (and therefore is an equality) for the trivial entropy flux pairs* $(\eta,q) := (\pm\tau, \mp v)$.

Adapting the results of [4], it is easy to show that any entropy $\eta(\tau,w)$ is convex in τ if and only if the associated entropy flux $q\equiv q(v)$ is concave (in v), and that there is an associated L^1 contraction principle "à la Kružkov," which implies the uniqueness. Consequently, we obtain the following.

THEOREM 6.4.

(i) *The sequence* $(U_h = (\tau_h, w_h))$ *in the hybrid model (given by the Godunov scheme* (2.9) *of the AR model and the Euler discretization* (3.3) *of the FLM model) is therefore a sequence of approximate weak entropy solutions to* (2.3)*, associated with the initial data* $U_h^0 = (\tau_h^0, w_h^0)$.

(ii) *Consequently, a subsequence* (U_h)*—in fact, by uniqueness, the whole sequence —converges to the unique weak entropy solution to* (2.3)*, with the same initial data.*

Proof. First, since $\partial_t\tau_h - \partial_X v_h = 0$, for $t_n < t < t_{n+1}$, for any smooth function $\phi(X,t)$ with compact support, we have

$$\begin{aligned}
&\int_0^\infty\int_{\mathbb{R}} (\tau_h\partial_t\phi - v_h\partial_X\phi)(X,t)dXdt + \int_{\mathbb{R}}\tau_h^0(X)\phi(X,0)dX\\
&= \sum_{n\geq 1}\sum_{i\in\mathbb{Z}}\left[\int_{I_i}\tau_h(X,t)\phi(X,t)dX\right]_{t_n^-}^{t_n^+} + \sum_i\int_{I_i}\tau_h^0(X)\phi(X,0)dX\\
&= \sum_{n\geq 1}\sum_{i\in\mathcal{M}^n}\int_{I_i}(\tau_h(X,t_n^-) - \tau_i^n)\phi(X,t_n)dX + \sum_{n\geq 1}\sum_{i\in\mu^n}\sum_{j=1}^N\int_{I_{ij}}(\tau_h(X,t_n^-) - \tau_{ij}^n)\phi(X,t_n)dX\\
&+ \sum_{i\in\mathcal{M}^n\cup\mu^n}\int_{I_i}\tau_h^0(X)\phi(X,0)dX =: A_h.
\end{aligned}$$

Now, since the test function ϕ is C^1 and compactly supported, using a Taylor expansion of ϕ on each interval, we get

$$|A_h| \leq (\Delta X)^2\,\|\partial_X\phi\|_{L^\infty}\sum_{n\geq 0}\sum_{i\in\mathcal{M}^n\cup\mu^n} TV_X(\tau_h(.,t);I_i)$$

$$\leq (\Delta X)^2 \frac{T}{\Delta t} \|\partial_X \phi\|_{L^\infty} \sup_{n \leq \frac{T}{\Delta t}} \sum_{i \in \mathcal{M}'' \cup \mu''} TV_X(\tau_h(.,t); I_i)$$

$$\leq \left(\frac{\Delta X}{\Delta t}\right) \Delta X T \|\partial_X \phi\|_{L^\infty} \sup_{n \leq \frac{T}{\Delta t}} \sum_{i \in \mathcal{M}'' \cup \mu''} TV_X(\tau_h(.,t); I_i)$$

$$= \left(\frac{\Delta X}{\Delta t}\right)^2 \Delta t T \|\partial_X \phi\|_{L^\infty} \sup_{n \leq \frac{T}{\Delta t}} \sum_{i \in \mathcal{M}'' \cup \mu''} TV_X(\tau_h(.,t); I_i).$$

Therefore, thanks to the BV estimates in Theorem 6.2, $|A_h| \longrightarrow 0$ as $\Delta t \longrightarrow 0$ (or $\Delta X \longrightarrow 0$), since $\frac{\Delta X}{\Delta t}$ is constant.

We proceed similarly with the entropy production term. On the one hand, the approximate solutions U_h are weak entropy solutions on any $[t_n, t_{n+1})$, and on the other hand, by Jensen's inequality, any convex entropy does not increase at time t_n in the Godunov averaging step as well as in the *macro-micro* or *micro-macro* synchronization. Consequently, for any entropy $\eta(\tau, w)$ convex with respect to τ, associated with the flux q, for all $\phi \in C_0^\infty(\mathbb{R} \times \mathbb{R}_+)$, $\phi \geq 0$, we have

$$\int_0^\infty \int_{\mathbb{R}} (\eta(U_h)\partial_t \phi + q(U_h)\partial_X \phi)(X,t) dX dt + \int_{\mathbb{R}} \eta(U_h(X,0))\phi(X,0) dX$$

$$\geq \sum_{n \geq 1} \sum_{i \in \mathcal{M}''} \int_{I_i} (\eta(U_h(X, t_n^-)) - \eta(U_i^n))\phi(X, t_n) dX$$

$$+ \sum_{n \geq 1} \sum_{i \in \mu''} \sum_{j=1}^{N} \int_{I_{i,j}} (\eta(u_h(X, t_n^-)) - \eta(u_{ij}^n))\phi(X, t_n) dX \geq 0. \qquad \square$$

Naturally, the above BV estimates are the crucial ingredient for showing the convergence of such a hybrid scheme to the unique globally defined weak entropy solution of a class of initial boundary value problems for a road with traffic light(s) or a road network in the spirit of [24] or [23]; see also [10]. We will investigate this in a forthcoming work.

7. Numerical simulations. In this section, we are concerned with the numerical investigation of the hybrid model. We consider the equations given by the explicit Euler time discretization of the microscopic model or equivalently the Godunov discretization of the macroscopic model in Lagrangian mass coordinates, which is itself equivalent to the Godunov discretization in Eulerian coordinates, in Lagrangian (moving) cells. We set the number of vehicles in the macroscopic cell to $N := 10$ and the length of a vehicle to $\Delta X := 5$ m. In order to show how information travels through the different parts of the hybrid model, we have fixed the MMR to a distance of 200 m (i.e., 100 m on both sides of the obstacle), which corresponds to the grey rectangle in Figures 7.1, 7.2, and 7.3. In order to get a better insight into the use of the hybrid model, we consider two scenarios and in each case we compare the densities given by the fully macroscopic model, the hybrid model, and the fully microscopic model.

The vertical line at $x = 0$ in Figures 7.1, 7.2, 7.3, and 7.5 is thickened to emphasize the state of the traffic light.

7.1. Case 1: The same time step in the whole hybrid scheme. This case corresponds exactly to the assumptions of the theoretical analysis of sections 5 and 6. We consider the same time step for the macroscopic and microscopic parts of the

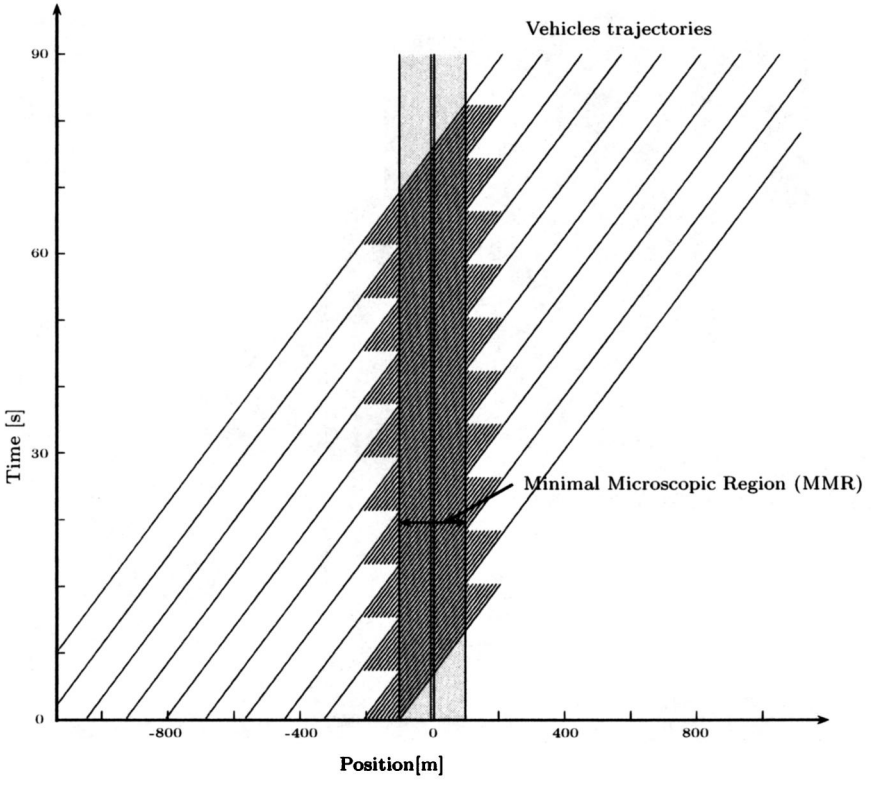

FIG. 7.1. *Case* 1. *The same time step in the microscopic and macroscopic regime: free flow traffic.*

hybrid model. Therefore, at time t_{n+1}, we have

$$\begin{cases} \tau_{ij}^{n+1} = \tau_{ij}^{n} + \frac{\Delta t}{\Delta X}\left(v_{ij-1}^{n} - v_{ij}^{n}\right), \\ w_{ij}^{n+1} = w_{ij}^{n} \end{cases} \tag{7.1}$$

in the microscopic part and

$$\begin{cases} \tau_{i}^{n+1} = \tau_{i}^{n} + \frac{\Delta t}{N\Delta X}\left(v_{i-1}^{n} - v_{ij}^{n}\right), \\ w_{i}^{n+1} = w_{i}^{n} \end{cases} \tag{7.2}$$

in the macroscopic part.

The time step Δt is chosen such that the CFL condition (2.8) is satisfied in both models. Obviously, the more drastic condition is the microscopic one, and thus we also expect too much numerical diffusion in the macroscopic part. For the simulations below the time step Δt is such that the Courant number is equal to 1 in the microscopic part.

The position of the vehicles is computed as follows:

$$x_{ij}^{n+1} = x_{ij}^{n} + \Delta t v_{ij}^{n}, \quad \text{with} \quad v_{ij}^{n} = w_{ij}^{n} - P(\tau_{ij}^{n}), \tag{7.3}$$

$$x_{i}^{n+1} = x_{i}^{n} + \Delta t v_{i}^{n}, \quad \text{with} \quad v_{i}^{n} = w_{i}^{n} - P(\tau_{i}^{n}). \tag{7.4}$$

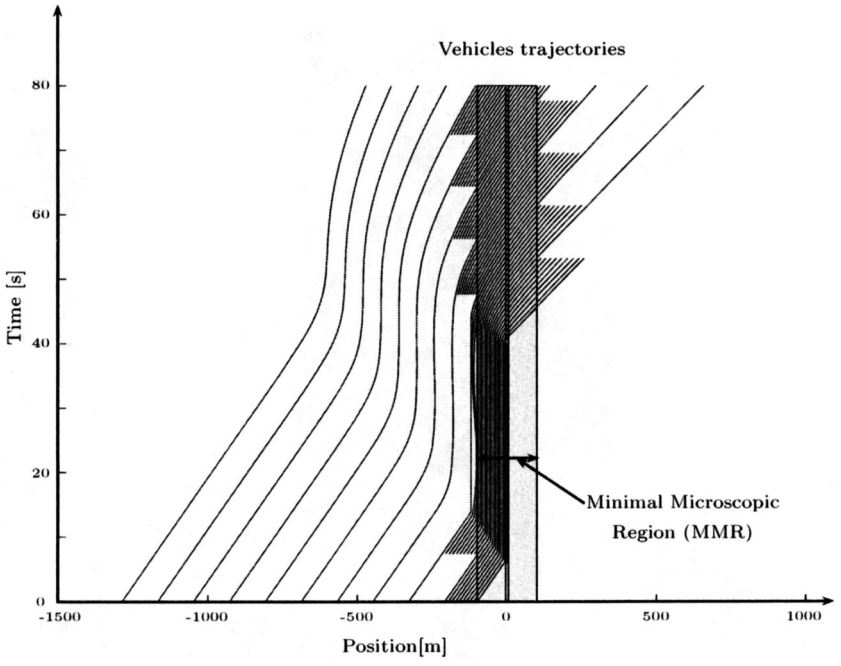

FIG. 7.2. *Case* 1. *The same time step in the microscopic and macroscopic regime: first a shock wave and then a rarefaction fan, both produced in the microscopic region, propagating backward in the macroscopic region.*

First, we simulate the hybrid model in a free flow situation. Trajectories of the "vehicles" in space and time for this case are plotted in Figure 7.1. In Figure 7.2, we plotted the "vehicles" trajectories when a "shock wave" appears at $t = 5$ s, followed by a "rarefaction fan" at $t = 40$ s in the minimal microscopic region (e.g., at a traffic light). Finally, Figure 7.3 shows the vehicles trajectories when a shock wave appears at $t = 40$ s followed by a rarefaction fan at $t = 70$ s, both downstream in the macroscopic regime (typically an incident on a highway). These "shocks" or "rarefaction waves" are produced numerically by forcing the leading vehicle to brake or accelerate. The simulations of these three situations show that the model synchronization does not perturb the wave propagation and allows for a nice description in each regime. In Figure 7.4, for the same situation (first a shock wave and then a rarefaction fan, both downstream of the minimal microscopic region), we plot the density for the fully macroscopic model, the hybrid model, and the fully microscopic model, respectively. The fully microscopic model gives a more precise description (but would be intractable for a large road network). In contrast, the description given by the macroscopic model is rather coarse to describe precisely the details in the minimal microscopic region. We also note that the shock is completely smoothed out by the numerical diffusion since the macroscopic CFL condition is $\frac{1}{10}$. Finally, the hybrid scheme gives an intermediate description, which is precise only in the region in which the details are important, in particular, here in the MMR $[-100$ m; $+100$ m$]$.

7.2. Case 2: Different time steps in the hybrid scheme. This case is not exactly covered by the assumptions of sections 5 and 6, even though the same ideas could in principle be extended to this situation. We consider different time steps in the two parts (microscopic part and macroscopic part) of the hybrid scheme, in order

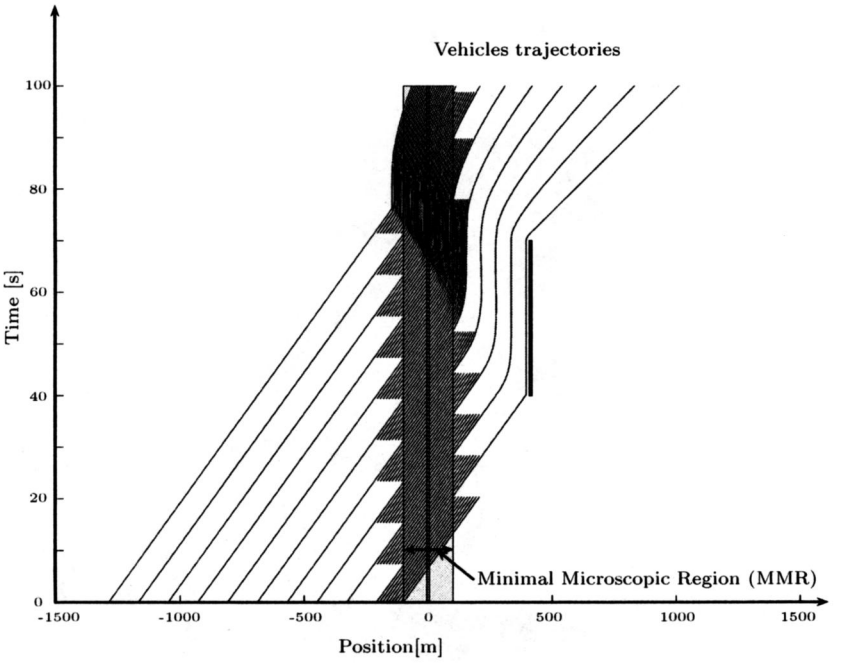

FIG. 7.3. *Case* 1. *The same time step in the microscopic and macroscopic regime: first a shock wave and then a rarefaction fan, both produced in the macroscopic region, propagating backward in the microscopic region.*

to have a Courant number (CFL condition) smaller than 1, but as large as possible in each region. Let Δt_{mic} and Δt_{mac} be, respectively, the time step in the microscopic part and the macroscopic part. In the microscopic region the updating takes place at each microscopic time $t_{n+1} = t_n + \Delta t_{\text{mic}}$, i.e.,

$$\begin{cases} \tau_{ij}^{n+1} = \tau_{ij}^n + \frac{\Delta t_{\text{mic}}}{\Delta X}\left(v_{ij-1}^n - v_{ij}^n\right), \\ w_{ij}^{n+1} = w_{ij}^n, \\ x_{ij}^{n+1} = x_{ij}^n + \Delta t_{\text{mic}} v_{ij}^n, \\ v_{ij}^{n+1} = w_{ij}^{n+1} - P(\tau_{ij}^{n+1}), \end{cases} \tag{7.5}$$

with Δt_{mic} chosen in such a way that the CFL condition (2.8) is satisfied in the microscopic model.

In contrast, in the macroscopic region, the updating takes place at each macroscopic time $\bar{t}_{n+1} = \bar{t}_n + \Delta t_{\text{mac}}$, i.e.,

$$\begin{cases} \tau_i^{n+1} = \tau_i^n + \frac{\Delta t_{\text{mac}}}{N\Delta X}\left(v_{i-1}^n - v_i^n\right), \\ w_i^{n+1} = w_i^n, \\ x_i^{n+1} = x_i^n + \Delta t_{\text{mac}} v_i^n, \\ v_i^{n+1} = w_i^{n+1} - P(\tau_i^{n+1}), \end{cases} \tag{7.6}$$

with Δt_{mac} chosen such that the CFL condition (2.8) is satisfied in the macroscopic model. Moreover, $\Delta t_{\text{mac}} = k\Delta t_{\text{mic}}$, with $1 < k \leq N$ and in general $k = N$.

One of the severe test cases is to handle the propagation of a strong shock, produced, e.g., at a (red) traffic light. In order to better track the propagation of this

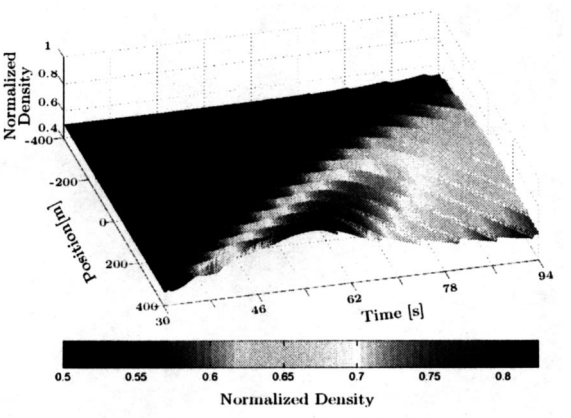

FIG. 7.4. *Case* 1. *The same time step in the microscopic and macroscopic regime: first a shock wave and then a rarefaction fan, both downstream from the minimal microscopic region* ([−100 m, 100 m]*):* (a) *the density in the macroscopic model,* (b) *the density in the hybrid model,* (c) *the density in the microscopic model.*

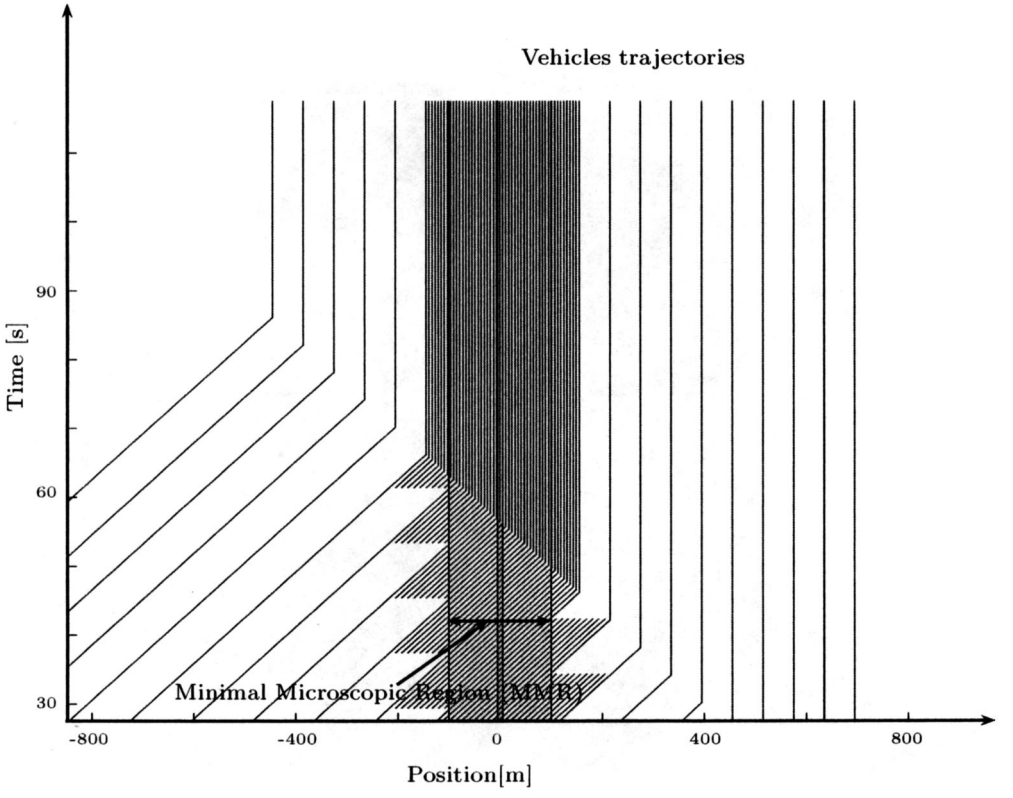

FIG. 7.5. *Case 2. Different time steps in the microscopic and macroscopic regime: a shock wave produced in the macroscopic region, propagating backward in the microscopic region.*

strong shock, we could use a front tracking method, which is a completely different numerical strategy. Here, we have used the following numerical procedure: At the macroscopic-microscopic interface, we include the following procedure to treat the case of a strong shock, as it happens at a traffic light. As soon as the last microscopic vehicle of a microscopic cell $(i-1)$ stops, the macroscopic cell i just behind this vehicle is tracked at each microscopic time step, until the time at which the "macroscopic vehicle" in cell i gets nose to tail with the microscopic vehicle ahead. Let t_s be this time. If t_s does not correspond to a macroscopic time, then we shift the macroscopic time step, not only for the macroscopic cell i but, exceptionally, for all the macroscopic cells behind cell i, which are updated at this time t_s using (once) the time step $\tilde{\Delta}t_{\text{mac}} = (t_s - \bar{t}_n)$, where $\bar{t}_n$ is the last macroscopic time before t_s. Thereafter, the time t_s becomes the beginning of the macroscopic time step for the cells behind cell i. We also recall that $\bar{t}_n \le t_s \le \bar{t}_n + \Delta t_{\text{mac}} = \bar{t}_{n+1}$.

For the numerical simulations plotted in Figures 7.5 and 7.6, we consider the CFL condition (2.8) with equality in both the microscopic and the macroscopic parts, and we set $\Delta t_{\text{mac}} = N\Delta t_{\text{mic}}$. As in the previous case, the fully microscopic model gives a more precise description (still too heavy for a large road network). In contrast, the description given by the macroscopic scheme is still a bit coarse to describe precisely the details in the MMR, but on the other hand, the shock is now much sharper even on this relatively coarse grid, thanks to the much better macroscopic CFL condition. Finally, the hybrid model gives an intermediate description which is very precise in the

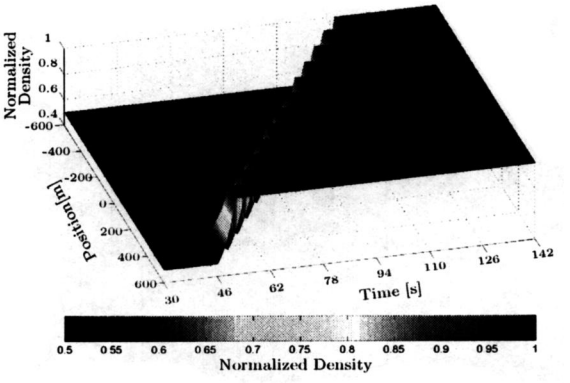

FIG. 7.6. *Case 2. Different time steps in the microscopic and macroscopic regime: a shock travelling from downstream to upstream coming from downstream of the minimal microscopic region ([−100 m, 100 m]): (a) the density in the macroscopic model, (b) the density in the hybrid model, (c) the density in the microscopic model.*

MMR and still tractable elsewhere. Note in particular that the numerical propagation speed of the shock is quite well preserved in each region.

8. Conclusion. Traffic investigation has simultaneously progressed both on the macroscopic and microscopic front. However, each description has its own limits. The recent success of hybrid models is due to their ability to capture traffic dynamics in a large domain with enough details near the obstacles.

In this paper, we propose a simple hybrid model based solely on a Lagrangian discretization of both the macroscopic and the microscopic models, coupled through Lagrangian interfaces periodically refreshed in order to *always* contain a fixed *Eulerian* region near an obstacle. As shown in the above numerical examples, the waves produced in either region nicely propagate through the other region. In particular, by this construction, the mass is automatically conserved through the interfaces.

This approach, which establishes a link between microscopic and macroscopic models and allows one to carry out simultaneous macro-micro simulations, could be hopefully a promising way to treat road intersections, in particular, on urban road networks.

REFERENCES

[1] B. Argall, E. Cheleshkin, J. M. Greenberg, C. Hinde, and P.-J. Lin, *A rigorous treatment of a follow-the-leader traffic model with traffic lights present*, SIAM J. Appl. Math., 63 (2002), pp. 149–168.

[2] A. Aw, A. Klar, T. Materne, and M. Rascle, *Derivation of continuum traffic flow models from microscopic follow-the-leader models*, SIAM J. Appl. Math., 63 (2002), pp. 259–278.

[3] A. Aw and M. Rascle, *Resurrection of "second order" models of traffic flow*, SIAM J. Appl. Math., 60 (2000), pp. 916–938.

[4] P. Bagnerini and M. Rascle, *A multiclass homogenized hyperbolic model of traffic flow*, SIAM J. Math. Anal., 35 (2003), pp. 949–973.

[5] C. Bardos, A. LeRoux, and J. Nedelec, *First order quasilinear equations with boundary conditions*, Comm. Partial Differential Equations, 4 (1979), pp. 1017–1043.

[6] E. Bourrel and J. B. Lessort, *Mixing microscopic and macroscopic representations of traffic flow: Hybrid model based on the Lighthill-Whitham–Richards theory*, Transportation Research Record, 1852 (2003), pp. 193–200.

[7] A. Bressan and H. K. Jenssen, *On the convergence of Godunov scheme for nonlinear hyperbolic systems*, Chinese Ann. Math. Ser. B, 21 (2000), pp. 269–284.

[8] W. Burghout, H. Koutsopoulos, and I. Andréasson, *Hybrid mesoscopic-microscopic traffic simulation*, Transportation Research Record, 1934 (2005), pp. 218–225.

[9] G.-Q. Chen, *Propagation and cancellation of oscillations for hyperbolic systems of conservation laws*, Comm. Pure Appl. Math., 44 (1991), pp. 121–140.

[10] G. M. Coclite, M. Garavello, and B. Piccoli, *Traffic flow on a road network*, SIAM J. Math. Anal., 36 (2005), pp. 1862–1886.

[11] C. M. Dafermos, *Hyperbolic Conservation Laws in Continuum Physics*, Springer-Verlag, Berlin, Heidelberg, New York, 2000.

[12] C. F. Daganzo, *The cell transmission model: A dynamic representation of highway traffic consistent with the hydrodynamic theory*, Trans. Res. B, 28 (1994), pp. 269–287.

[13] C. F. Daganzo, *Requiem for second order fluid approximations of traffic flow*, Trans. Res. B, 29 (1995), pp. 277–286.

[14] R. J. Diperna, *Measure-valued solutions to conservation laws*, Arch. Rational Mech. Anal., 88 (1985), pp. 223–270.

[15] D. C. Gazis, R. Herman, and R. W. Rothery, *Nonlinear follow-the-leader models of traffic flow*, Oper. Res., 9 (1961), pp. 545–567.

[16] E. Godlewsky and P. A. Raviart, *Numerical Approximation of Hyperbolic Systems of Conservation Laws*, Appl. Math. Sci. 118, Springer-Verlag, New York, 1996.

[17] S. K. Godunov, *A difference method for numerical calculation of discontinuous solutions of the equations of hydrodynamics*, Mat. Sb. (N.S.), 47 (1959), pp. 271–306.

[18] J. M. Greenberg, *Extensions and amplifications of a traffic model of Aw and Rascle*, SIAM J. Appl. Math., 62 (2001), pp. 729–745.

[19] D. HELBING, A. HENNECKE, V. SHVETSOV, AND M. TREIBER, *Micro- and macro-simulation of freeway traffic*, Math. Comput. Modelling, 35 (2002), pp. 517–547.
[20] D. HELBING AND M. TREIBER, *Critical discussion of "synchronized flow,"* Cooper@tive Tr@nsport@tion Dyn@mics, 1 (2002), pp. 2.1.–2.24.
[21] A. HENNECKE, M. TREIBER, AND D. HELBING, *Macroscopic simulations of open systems and micro-macro link*, in Traffic and Granular Flow '99, D. Helbing, H. J. Herrmann, M. Schreckenberg, and D. E. Wolf, eds., Springer, Berlin, 2000, pp. 383–388.
[22] R. HERMAN AND I. PRIGOGINE, *Kinetic Theory of Vehicular Traffic*, American Elsevier, New York, 1971.
[23] M. HERTY, S. MOUTARI, AND M. RASCLE, *Optimization criteria for modelling intersections of vehicular traffic flow*, Netw. Heterog. Media, 1 (2006), pp. 275–294.
[24] M. HERTY AND M. RASCLE, *Coupling conditions for a class of second-order models for traffic flow*, SIAM J. Math. Anal., 38 (2006), pp. 595–616.
[25] H. HOLDEN AND N. H. RISEBRO, *A mathematical model of traffic flow on a network of unidirectional roads*, SIAM J. Math. Anal., 26 (1995), pp. 999–1017.
[26] S. N. KRUŽKOV, *First order quasilinear equations with several independent variables*, Math. USSR-Sb., 10 (1970), pp. 217–243.
[27] J. LAVAL AND C. F. DAGANZO, *Lane-changing in traffic streams*, Trans. Res. B, 40 (2006), pp. 251–264.
[28] J. P. LEBACQUE, *Les modèles macroscopiques du traffic*, Ann. des Ponts, 67 (1993), pp. 24–45.
[29] J. P. LEBACQUE, *The Godunov scheme and what it means for first order traffic flow models*, in Transportation and Traffic Theory, J. B. Lessort, ed., Pergamon Press, Oxford, UK, 1996, pp. 647–678.
[30] M. LIGHTHILL AND J. WHITHAM, *On kinematic waves*, Proc. Roy. Soc. London Ser. A, 229 (1955), pp. 281–345.
[31] L. MAGNE, S. RABUT, AND J. F. GABARD, *Towards an hybrid macro-micro traffic flow simulation model*, in Proceedings of the INFORMS Spring Meeting, Salt Lake City, UT, 2000.
[32] R. NATALINI, *Convergence to equilibrium for the relaxation approximations of conservation laws*, Comm. Pure Appl. Math., 49 (1996), pp. 795–823.
[33] H. PAYNE, *FREFLO: A macroscopic simulation model for freeway traffic*, Transportation Research Record, 722 (1979), pp. 68–75.
[34] L. TONG, *Well-posedness theory of an inhomogeneous traffic flow model*, Discrete Contin. Dyn. Syst. Ser. B, 2 (2002), pp. 401–414.
[35] D. H. WAGNER, *Equivalence of the Euler and Lagrangian equations of gas dynamics for weak solutions*, J. Differential Equations, 68 (1987), pp. 118–136.
[36] G. C. K. WONG AND S. C. WONG, *A multi-class traffic flow model—an extension of LWR model with heterogeneous drivers*, Trans. Res. A, 36 (2002), pp. 827–841.
[37] H. M. ZHANG, *A non-equilibrium traffic model devoid of gas-like behaviour*, Trans. Res. B, 36 (2002), pp. 275–298.